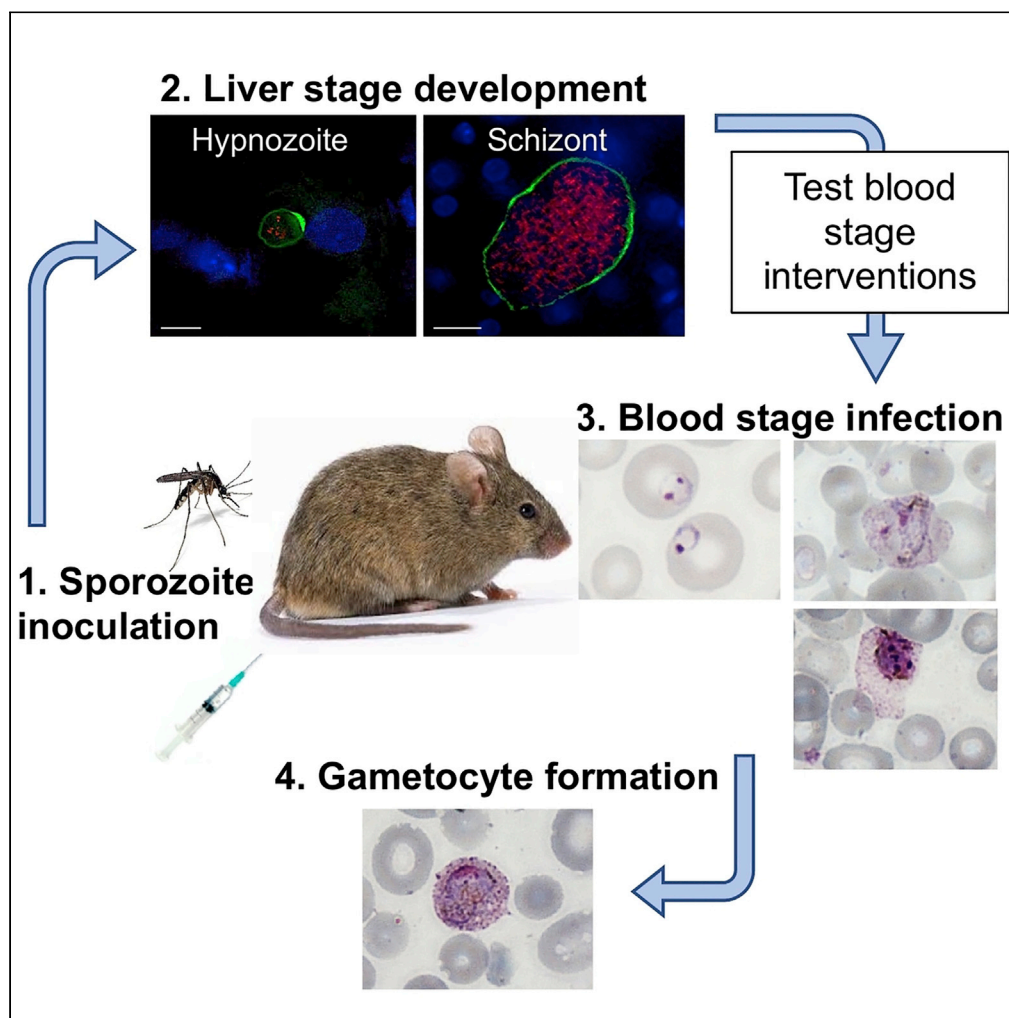


## Article

A Humanized Mouse Model for *Plasmodium vivax* to Test Interventions that Block Liver Stage to Blood Stage Transition and Blood Stage Infection

Carola Schäfer,  
Wanlapa  
Roobsoong, Niwat  
Kangwanrangan, ...,  
Jetsumon  
Sattabongkot,  
Sebastian A.  
Mikolajczak, Stefan  
H.I. Kappe

stefan.kappe@  
seattlechildrens.org

**HIGHLIGHTS**

A humanized mouse model allows *P. vivax* liver stage to blood stage transition

This model is highly suitable to test *P. vivax* blood stage interventions *in vivo*

*P. vivax* parasites can commit to sexual development as they emerge from the liver

## Article

A Humanized Mouse Model for *Plasmodium vivax* to Test Interventions that Block Liver Stage to Blood Stage Transition and Blood Stage Infection

Carola Schäfer,<sup>1</sup> Wanlapa Roobsoong,<sup>2</sup> Niwat Kangwanrangsan,<sup>3</sup> Martino Bardelli,<sup>4</sup> Thomas A. Rawlinson,<sup>4</sup> Nicholas Dambrauskas,<sup>1</sup> Olesya Trakhimets,<sup>1</sup> Chaitra Parthiban,<sup>5</sup> Debashree Goswami,<sup>1</sup> Laura M. Reynolds,<sup>1</sup> Spencer Y. Kennedy,<sup>1</sup> Erika L. Flannery,<sup>1,8</sup> Sean C. Murphy,<sup>5</sup> D. Noah Sather,<sup>1,6,7</sup> Simon J. Draper,<sup>4</sup> Jetsumon Sattabongkot,<sup>2</sup> Sebastian A. Mikolajczak,<sup>1,8</sup> and Stefan H.I. Kappe<sup>1,6,7,9,\*</sup>

## SUMMARY

**The human malaria parasite *Plasmodium vivax* remains vastly understudied, mainly due to the lack of suitable laboratory models. Here, we report a humanized mouse model to test interventions that block *P. vivax* parasite transition from liver stage infection to blood stage infection. Human liver-chimeric FRGN huHep mice infected with *P. vivax* sporozoites were infused with human reticulocytes, allowing transition of exo-erythrocytic merozoites to reticulocyte infection and development into all erythrocytic forms, including gametocytes, *in vivo*. In order to test the utility of this model for preclinical assessment of interventions, the invasion blocking potential of a monoclonal antibody targeting the essential interaction of the *P. vivax* Duffy Binding Protein with the Duffy antigen receptor was tested by passive immunization. This antibody inhibited invasion by over 95%, providing unprecedented *in vivo* evidence that PvDBP constitutes a promising blood stage vaccine candidate and proving our model highly suitable to test blood stage interventions.**

## INTRODUCTION

*Plasmodium vivax* (*P. vivax*) and *Plasmodium falciparum* (*P. falciparum*) are the leading causes of malaria worldwide, putting nearly half the world's population at risk of infection. *P. falciparum* causes the majority of malaria-associated morbidities and mortalities in sub-Saharan Africa, whereas *P. vivax* is geographically most widespread (Gething et al., 2011; Shretta et al., 2017). Its endemicity throughout tropical as well as temperate climate zones is attributed to the parasite's ability to form dormant liver stages, hypnozoites, which can activate weeks or months after the primary infection, leading to repeated onset of blood stage infection and recurring transmission (Adams and Mueller, 2017; White et al., 2014; White, 2011).

The establishment of a continuous *in vitro* culture system for the blood stages of *P. falciparum* more than 40 years ago (Trager, 1977) has revolutionized insights into parasite biology and malaria pathogenesis, allowing genetic manipulation (Goswami et al., 2019) as well as extensive omics studies (Cowell and Winzeler, 2019) and evaluation of novel interventions (Cowell and Winzeler, 2019; Mogire et al., 2017). In contrast, research on *P. vivax* greatly lags behind and despite more than a century of efforts (Bass and Johns, 1912; Noulin et al., 2013), a continuous *in vitro* culture system has yet to be established. Unlike *P. falciparum*, which infects red blood cells (RBCs) of all stages of maturity, *P. vivax* preferentially, if not exclusively, infects reticulocytes expressing the surface marker CD71 (Gruszczyk et al., 2018; Malleret et al., 2015). These cells are produced in the bone marrow and released into circulation as they mature, where they constitute only 0.5% to 1.5% of all RBCs (Ney, 2011). Reticulocytes can be enriched by magnetic beads or density gradient centrifugation, but robust growth of *P. vivax* parasites even in pure reticulocyte preparations cannot routinely be observed *in vitro* (Bermudez et al., 2018).

The lack of an *in vitro* culture system also prevents the generation of gametocytes, limiting our current knowledge of *P. vivax* gametocytogenesis. Since the full *P. vivax* life cycle cannot be maintained in the

<sup>1</sup>Center for Global Infectious Disease Research, Seattle Children's Research Institute, Seattle, WA 98109, USA

<sup>2</sup>Mahidol Vivax Research Unit, Faculty of Tropical Medicine, Mahidol University, Bangkok 10400, Thailand

<sup>3</sup>Department of Pathobiology, Faculty of Science, Mahidol University, Bangkok 10400, Thailand

<sup>4</sup>The Jenner Institute, University of Oxford, Oxford OX3 7DQ, UK

<sup>5</sup>Departments of Laboratory Medicine and Microbiology and Center for Emerging and Re-emerging Infectious Diseases, University of Washington, Seattle, WA 98109, USA

<sup>6</sup>Department of Pediatrics, University of Washington, Seattle, WA 98105, USA

<sup>7</sup>Department of Global Health, University of Washington, Seattle, WA 98105, USA

<sup>8</sup>Present address: Novartis Institute for BioMedical Research, Novartis Institute for Tropical Diseases, Emeryville, CA 94608, USA

<sup>9</sup>Lead Contact

\*Correspondence: stefan.kappe@seattlechildrens.org

<https://doi.org/10.1016/j.isci.2020.101381>



laboratory, research relies on patient samples. This is a great obstacle for any *P. vivax* research and largely limits the progress that can be achieved in the field. Furthermore, it necessitates the use of a different field isolate for every experiment, complicating assay optimization and often leading to great inter-experimental variation due to differences between the strains. Clearly, the lack of a continuous *in vitro* culture system impedes basic research on *P. vivax* erythrocytic stages and there is an urgent need for relevant models to test disease interventions.

Recently, the use of human liver-chimeric mice has opened up new avenues for research on *P. vivax* liver stages. *Fah<sup>-/-</sup>Rag2<sup>-/-</sup>IL2rg<sup>-/-</sup>* mice transplanted with primary human hepatocytes (FRG KO huHep) (Azuma et al., 2007) are highly susceptible to infection with *P. vivax* sporozoites and support full *P. vivax* liver stage development as well as the formation and activation of hypnozoites (Mikolajczak et al., 2015). Backcrossing of FRG mice to the non-obese diabetic (NOD) background (FRGN KO) additionally makes these mice more suitable for repopulation with human red blood cells. This increased tolerance of human cells is due to a NOD strain-derived polymorphism in the signal-regulatory protein alpha (SIRP $\alpha$ ), leading to improved engagement of SIRP $\alpha$  expressed on mouse phagocytes with its ligand CD47, ubiquitously expressed on the transferred human cells, thereby providing a more efficient “don’t-eat-me signal” (Kwong et al., 2014; Yamauchi et al., 2013).

Here, we show that FRGN KO huHep mice support *P. vivax* liver stage development with formation of exo-erythrocytic merozoites that efficiently infect infused human reticulocytes, allowing reproducible transition from liver stage infection to blood stage infection. We provide evidence that this model fills the gap of an urgently needed small animal model that allows testing of *P. vivax* erythrocytic stage interventions.

## RESULTS

### Successful Transition of *P. vivax* Liver Stage Parasites to Blood Stage Parasites

A pivotal transition point in the malaria life cycle occurs when parasites emerging from the liver infect the first red blood cells. We have shown previously that *P. vivax* liver stage development in FRG KO huHep mice is completed 9–10 days post sporozoite infection and culminates with the release of exo-erythrocytic merozoites from the liver into the blood stream (Mikolajczak et al., 2015). Here, we developed this model further in order to allow exo-erythrocytic merozoite infection of reticulocytes and asexual blood stage development. We modified our protocol previously developed for *P. falciparum* (Foquet et al., 2018) using immunomodulation with Clodronate liposomes and Cyclophosphamide to deplete mouse macrophages and mouse neutrophils, respectively, which prevents clearance of infected human red blood cells. We combined this immunomodulation protocol in FRGN KO huHep mice with intravenous (i.v.) injections of enriched human reticulocyte preparations on days 9 and 10 post *P. vivax* sporozoite infection (Figure 1A). In order to also decrease the potential innate immune response in the host that is caused by liver infection (Liehl et al., 2015; Miller et al., 2014), Clodronate Liposomes and Cyclophosphamide were injected intraperitoneally (i.p.) on days 3 and 7 post infection.

We first assessed whether this protocol supports liver infection and transition of *P. vivax* exo-erythrocytic merozoites to blood stage infection using either i.v. injection of sporozoites or infection by mosquito bite, the latter to test whether the natural route of infection is feasible with *Anopheles dirus* (*An. dirus*) mosquitoes. In addition, we directly assessed the benefits of the immunomodulation with Clodronate liposomes and Cyclophosphamide. We infected a cohort of eleven FRGN KO huHep mice with *P. vivax* sporozoites. Eight FRGN KO huHep mice were i.v. infected with 0.9 million sporozoites isolated from *An. dirus* salivary glands. Four FRGN KO huHep mice were treated with Clodronate liposomes and Cyclophosphamide, whereas the other group of four mice remained untreated prior to reticulocyte injection. Three additional FRGN KO huHep mice were infected by the bites of 50 *P. vivax*-infected *An. dirus* mosquitoes and treated with Clodronate liposomes and Cyclophosphamide as described above.

On day 10 post infection, 4 hours after the second reticulocyte injection, asexual blood stage parasites could be detected on Giemsa-stained thin blood smears of all i.v.-infected FRGN KO huHep mice and, notably, also in the FRGN KO huHep mice infected by mosquito bite. At this time point, parasitemia as high as 2% was observed in the group infected intravenously and treated with Clodronate liposomes and Cyclophosphamide. The immunomodulatory treatment significantly increased the amount of parasite 18S RNA detected by qRT-PCR over the untreated group, supporting the benefit of this treatment (Figure 1B). Therefore, this protocol was used for all further experiments. Levels of human red blood cell

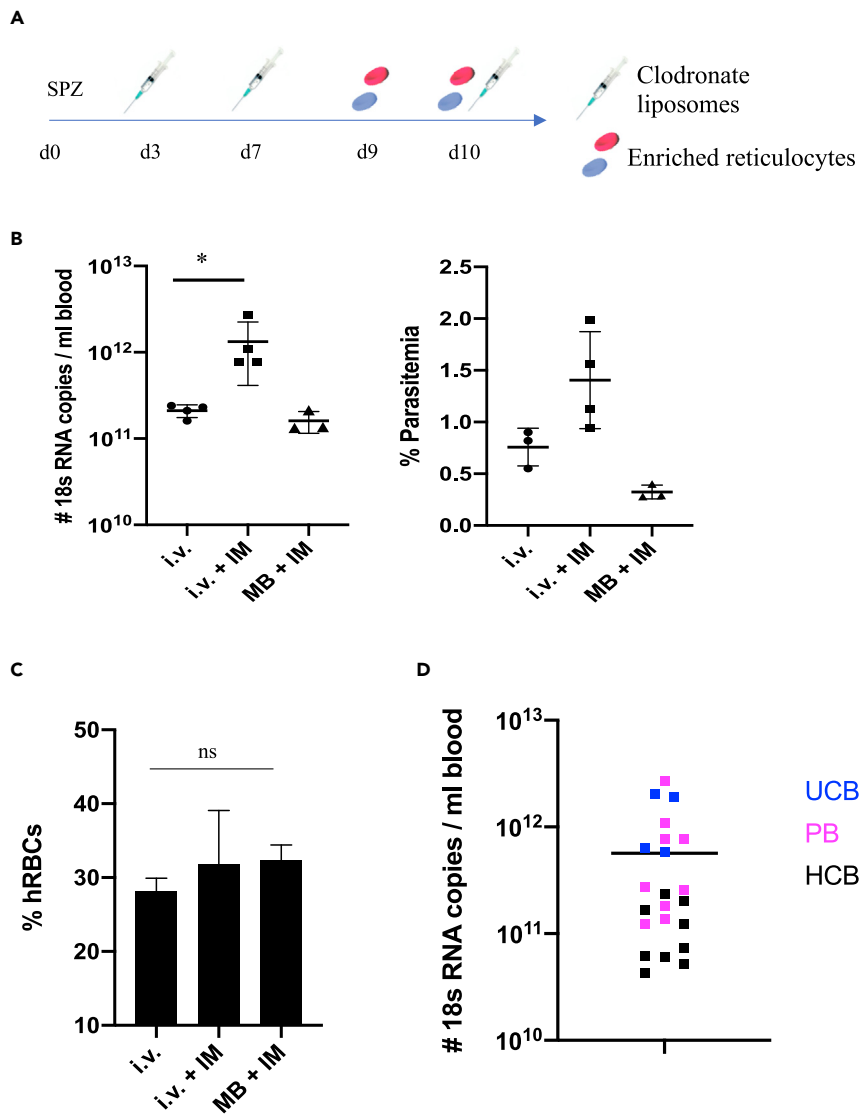


### Figure 1. Reticulocyte Invasion by Exo-Erythrocytic Merozoites

(A) FRGN KO huHep mice were infected with *P. vivax* sporozoites either by intravenous injection of salivary gland sporozoites or by mosquito bite (50 mosquitos per mouse). Three days post infection, mice received 150  $\mu$ L Clodronate liposomes and 150 mg/kg Cyclophosphamide intraperitoneally. These injections were repeated on days 7 and 10 post infection. On days 9 and 10 post infection, 400  $\mu$ L enriched human reticulocytes at 50% hematocrit was injected intravenously to provide a pool of target cells for parasites egressing from the liver.

(B) Mice were randomized into three groups of which two groups were infected by injection of 0.9 million sporozoites (i.v.) and one group was infected by the bite of 50 mosquitos (MB). One group did not receive any immunomodulation (IM). *P. vivax* 18S RNA was measured by qRT-PCR, and parasitemia was counted on thin blood smears 5 h after the second reticulocyte injection. Parasites were detected in all groups, and the i.v. + IM protocol led to a significant increase in parasites detected. Each dot represents one mouse. Shown is mean  $\pm$  SD. Statistics: Mann-Whitney test; \*p = 0.0286.

(C) IFAs were performed on thin blood smears staining for human Glycophorin A. Thousand cells were counted per slide and the percentage of human red blood cells was calculated. No significant difference between the groups was observed. Shown is mean  $\pm$  SD.

(D) The copy number of *P. vivax* 18S RNA measured by qRT-PCR 5 h after the second reticulocyte injection is shown for five independent experiments. The different blood sources used are marked in different colors. Parasites were detected in every mouse analyzed, independent of the blood source used. Mean is shown.

UCB, umbilical cord blood; PB, peripheral blood; HCB, blood from patients with hemochromatosis.

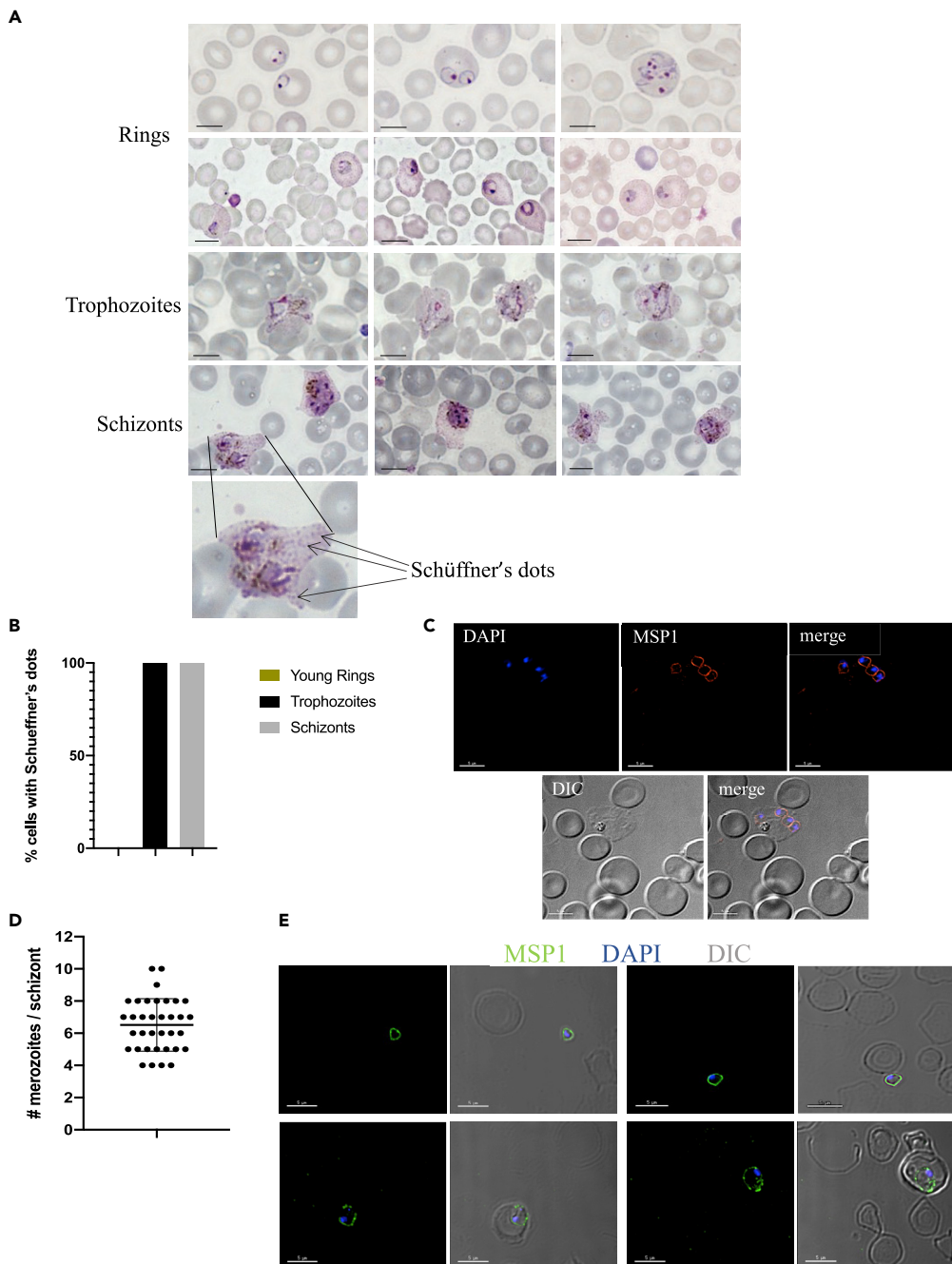


**Figure 2. Asexual Blood Stage Parasite Morphology in FRGN KO huHep Mice**

(A) Mice were infected with *P. vivax* sporozoites, and parasites were transitioned to blood stages following the protocol described in Figure 1A. Giemsa-stained thin blood smears were analyzed at various time points between day 9 (5 h after the first reticulocyte injection) and day 12 post infection. All asexual parasite forms were seen, and the morphology was comparable with parasites seen on blood smears from *P. vivax*-infected patients. Scale bars represent 5  $\mu$ m.

(B) Host cells infected with parasites at different developmental stages, including early ring stages 4 h after the first reticulocyte infection and mature schizonts, were analyzed for the presence of Schuffner's dots. None of the early ring stage-infected reticulocytes showed any Schuffner's dots, whereas these were observed on all trophozoite and schizont-infected cells.

(C) IFAs were performed on thin blood smears from day 12 post infection and stained with anti-MSP1 and DAPI. Intact MSP1 staining of fully segmented schizonts could be observed. Scale bars represent 5  $\mu$ m.

**Figure 2. Continued**

(D) Thin blood smears from two individual experiments were stained with anti-MSP1 and DAPI. The quantity of merozoites per schizont was counted. On average, 6.5 merozoites per schizont were detected. Each dot represents one schizont. Mean  $\pm$  SD is shown.

(E) IFAs were performed on thin blood smears from day 14 post infection and stained with anti-MSP1 and DAPI. Free merozoites as well as invaded ring stage parasites were observed. Scale bars represent 5  $\mu$ m.

(hRBC) reconstitution were comparable between the groups, reaching more than 30% blood chimerism after the second reticulocyte injection (Figure 1C). Notably, the significantly lower blood stage parasitemia observed in the group of mice not receiving any immunomodulation was not caused by increased clearance of all hRBCs, indicating a selective clearance of infected hRBCs by phagocytic cells and neutrophils.

*P. vivax* parasites preferentially, if not exclusively, infect reticulocytes and not mature RBCs. This necessitates the enrichment of large volumes of these rare cells. We therefore set out to determine the most suitable source of reticulocytes. We used three different sources of blood, namely, peripheral blood from healthy donors, umbilical cord blood as well as peripheral blood from patients with hemochromatosis. Peripheral blood from healthy donors has low reticulocyte counts ( $\sim$ 0.5%), whereas reticulocyte counts in umbilical cord blood can reach up to 5%. Patients with hemochromatosis, an iron-overload disease, undergo frequent phlebotomy as their standard treatment, which over time leads to increased reticulocyte counts of around 3%. Reticulocytes were enriched by density gradient centrifugation, which yielded red blood cell preparations containing 30%–60% reticulocytes, as determined by New Methylene Blue staining. In each of five independent experiments using different reticulocyte sources and following the protocol depicted in Figure 1A, *P. vivax* asexual blood stage parasites were consistently seen on thin blood smears on days 9 and 10 post sporozoite infection and high levels of *P. vivax* 18S RNA were detected by qRT-PCR independent of the reticulocyte source used (Figure 1D). Throughout these experiments, a total of 22 FRGN KO huHep mice and five different *P. vivax* field isolates were used. The protocol described here therefore allows efficient and reproducible transition of *P. vivax* field isolates from liver stage infection to blood stage infection.

***P. vivax* Asexual Blood Stages Develop Normally in FRGN KO huHep/huRetic Mice**

Next, we wanted to assess whether the *P. vivax* exo-erythrocytic merozoites released from the liver of FRGN KO huHep mice could initiate normal intra-erythrocytic development. We performed Giemsa stains of thin blood smears at various time points after transition, and all asexual parasite forms could be detected between days 9 and 12 post infection. Typical morphological features described for *P. vivax*-infected RBCs from human infections (Adams and Mueller, 2017; Aikawa et al., 1975; Suwanarusk et al., 2004) were readily observed: red blood cells infected by multiple ring stage parasites; Schüffner's dots; an increase in size and deformation of the infected RBC, leading to the typical ameboid shape (Figure 2A). Host cells infected with parasites at different developmental stages, including early ring stages 4 h after the first reticulocyte infection and mature schizonts, were analyzed for the presence of Schüffner's dots. None of the early ring stage-infected reticulocytes showed the development of Schüffner's dots, whereas these were observed on all trophozoite and schizont-infected cells (Figure 2B). Schizonts were detected at 50 h after the first reticulocyte injection, indicating that the parasites developed within their normal 48-h life cycle. In order to investigate whether schizonts mature fully and release infectious merozoites, we performed immunofluorescence assays (IFAs) using antibodies against merozoite surface protein 1 (MSP1). This staining revealed fully segmented schizonts (Figure 2C). The number of merozoites per schizont was quantified, and on average, a schizont contained 6.5 merozoites (Figure 2D). Remarkably, free merozoites as well as invaded ring stage parasites could be detected as late as day 14 post infection (5 days post first reticulocyte injection), indicating the release of infectious erythrocytic merozoites and the subsequent invasion of new target red blood cells (Figure 2E).

In order to confirm that the merozoites exclusively infect red blood cells of human origin, we performed IFAs using antibodies to the parasite marker BiP and the human RBC marker CD235a. We examined 50 infected RBCs at different time points post transition. At any time point, parasites were exclusively found in CD235a-positive cells (Figure 3A), indicating that no successful invasion of mouse RBCs had occurred.

We further utilized the FRGN KO huHep/huRetic model to investigate *P. vivax* gametocytogenesis *in vivo*. IFAs on liver sections from *P. vivax* sporozoite-infected FRG KO huHep mice revealed a subset of exo-erythrocytic schizonts that stained positive for the immature gametocyte marker Pvs16, 9 days post infection

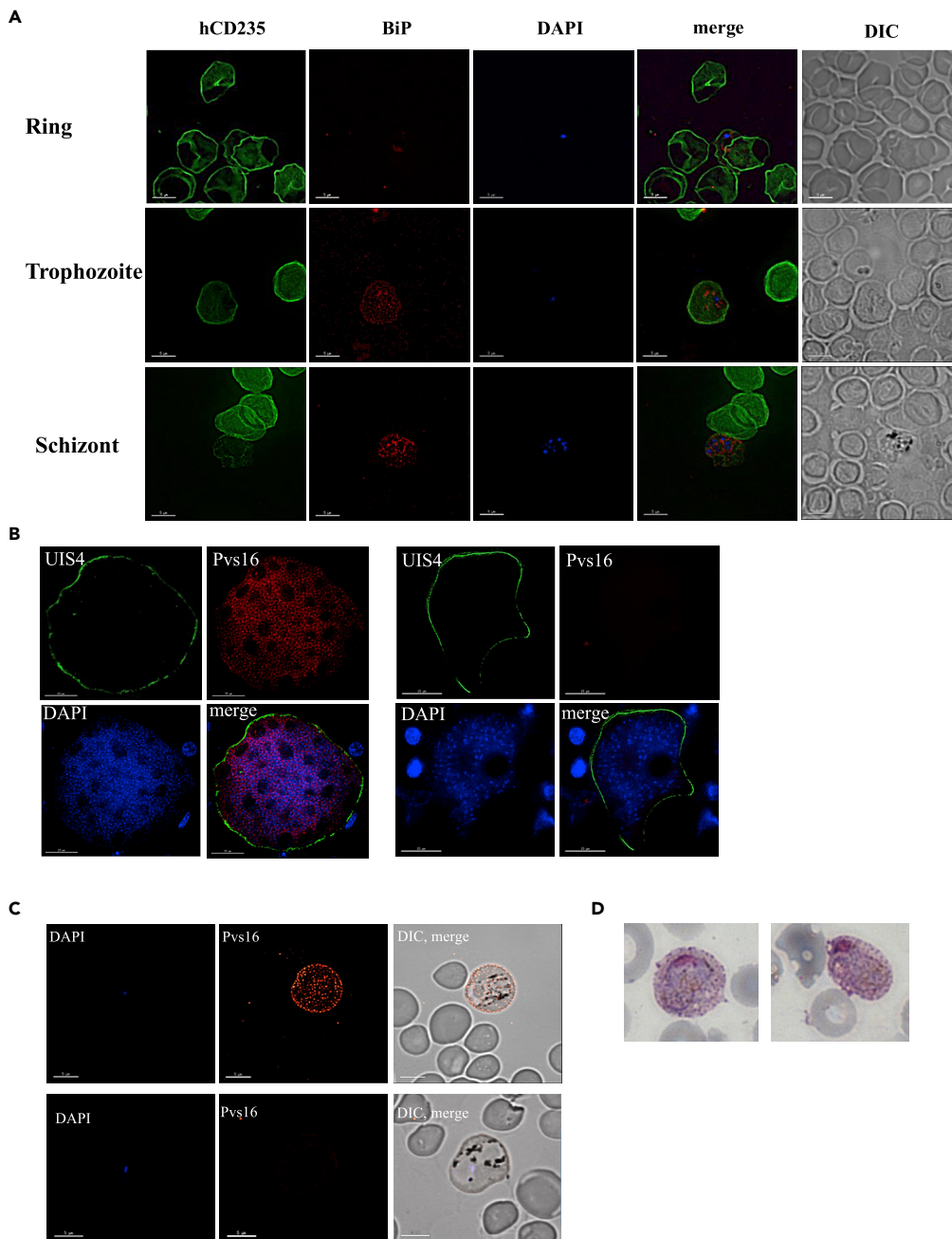


**Figure 3. Parasites Exclusively Infect Human Red Blood Cells and a Subset of Parasites Express the Gametocyte Antigen Pvs16**

(A) To determine whether parasites can also be observed in mouse red blood cells, thin blood smears from different time points post infection were stained with anti-CD235a and anti-BiP, a parasite protein located in the endoplasmic reticulum. Nucleic acid was visualized with DAPI. Fifty infected cells were imaged, and all parasite forms were only detected in human cells. Scale bars represent 5  $\mu$ m.

(B) Liver sections from day 9 post sporozoite infection were stained for Pvs16, and a subset of exoerythrocytic schizonts expressing this gametocyte antigen was observed. Scale bars represent 15  $\mu$ m.

(C) IFAs were performed on thin blood smears from day 11 post infection; staining for Pvs16 and a subset of parasites expressing this gametocyte marker was detected. Scale bars represent 5  $\mu$ m.

(D) Gametocytes were detected on Giemsa-stained thin blood smears.

See also [Figure S1](#).

(Figure 3B). In contrast, IFAs staining for the mature gametocyte marker and one of the leading candidate antigens for a transmission blocking vaccine, Pvs230, revealed no expression (data not shown). In order to confirm these findings, we performed RT-PCR using RNA isolated from *P. vivax* sporozoite-infected FRG KO huHep livers 8 days post infection. We successfully amplified Pvs16, but not Pvs230, confirming the results obtained by IFAs (Figure S1). IFAs on blood smears obtained 11 days post sporozoite infection, approximating a time point  $\leq 2$  days post onset of blood stage infection, also revealed a subset of parasites expressing Pvs16 (Figure 3C), indicating the presence of sexual stages very early post onset of blood stage parasitemia. This presence of gametocytes was confirmed by Giemsa-stained thin blood smears (Figure 3D).

### Inhibition of Reticulocyte Invasion by an Antibody Targeting the Essential *P. vivax* Duffy Binding Protein Interaction with Its Receptor

Assays currently available to test interventions targeting *P. vivax* asexual blood stages are extremely limited (Armistead and Adams, 2018), and no small animal model has been developed for this purpose. In order to assess whether the FRGN KO huHep/huRetic model can fill this gap, we measured the *in vivo* invasion-inhibitory efficacy of a candidate antibody biologic targeting the essential interaction between *P. vivax* Duffy Binding Protein (PvDBP) and its receptor the Duffy Antigen Receptor for Chemokines (DARC). PvDBP is the leading blood stage vaccine candidate for this parasite species (Singh et al., 2018). It has previously been shown that immunization with the receptor binding domain of PvDBP (PvDBPII) leads to the generation of antibodies that can inhibit the interaction between recombinant DBP and recombinant DARC (de Cassan et al., 2015; Grimberg et al., 2007; Moreno et al., 2008; Payne et al., 2017; Singh et al., 2018). Furthermore, the presence of high-level PvDBPII-specific binding inhibitory antibodies after natural infection is associated with protection against *P. vivax* infection (He et al., 2019; King et al., 2008). In a recent study, ten human monoclonal antibodies (mAbs) from a PvDBP-immunized volunteer were cloned and tested for their blocking activity using the DBP-DARC interaction. One mAb potently inhibited invasion *in vitro* using *P. knowlesi* parasites expressing *P. vivax* DBP (Rawlinson et al., 2019).

Here we tested a version of this antibody ("anti-PvDBP") for invasion-inhibitory activity against *P. vivax* merozoites *in vivo*, whereby we infected eight FRGN KO huHep mice i.v. with 0.8 million *P. vivax* sporozoites. Mice were randomized into two groups with four mice each. We followed our protocol described above and outlined in Figure 4A. On day 8 post infection and 24 h before the first reticulocyte injection, each group was passively transferred with 100 mg/kg of anti-PvDBP mAb, a control antibody or PBS. Serum antibody levels were measured immediately before the first reticulocyte injection and revealed high serum concentrations of mAb (Figure S2). Giemsa-stained thin blood smears were generated 5 and 24 h after the second reticulocyte injection, and the number of parasites within 50 fields of view was quantified by microscopy (Figure 4B). Strikingly, PvDBP mAb showed potent inhibition of *P. vivax* RBC invasion, with no intracellular parasites observed in this group of mice, in contrast to the control group in which on average 67.5 intracellular parasites were observed. During the course of the infection, two of the four mice from this group remained blood smear negative and only a single parasite each was seen on the remaining two mice. There was no significant difference in the level of red blood cell chimerism between the groups (Figure 4C).

This experiment demonstrates that the FRGN KO huHep/huRetic mouse model is suitable to test *P. vivax* intervention strategies *in vivo*, thereby complementing the currently available assays with an urgently needed small animal model. It is the only model in which interventions can be tested against the first wave of merozoites egressing from the liver, the parasite population that constitutes the essential transition from liver to blood and that a vaccine will have to target in order to prevent onset of blood stage infection, clinical disease, and onward parasite transmission.

## DISCUSSION

Research on *P. vivax* erythrocytic stages is greatly impeded by the lack of a continuous *in vitro* culture system and robust preclinical models to assess interventions. Here, we report the development of the first small animal model for investigation of *P. vivax* blood stage interventions. Liver-chimeric FRGN KO huHep mice were infected using the natural route by mosquito bite or i.v. injection of salivary gland sporozoites. Liver stage development and exo-erythrocytic schizogony resulted in the release of exo-erythrocytic merozoites that were able to infect infused human reticulocytes. This is the only model that recapitulates the parasite's physiological developmental cycle, combining sporozoite infection by mosquito bite and full

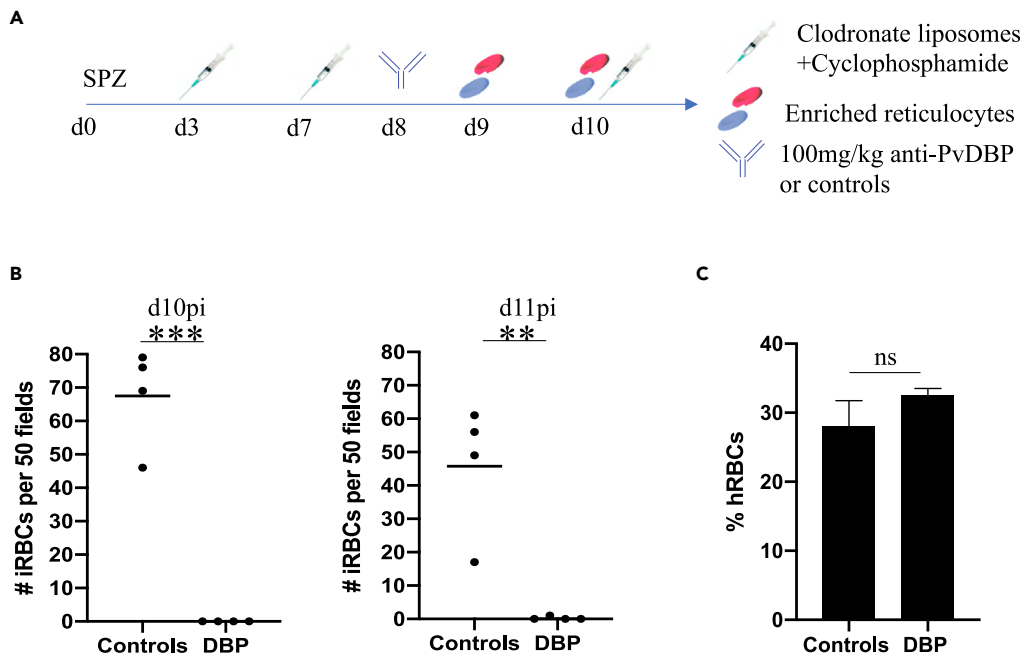


**Figure 4. Inhibition of Invasion by a Monoclonal Antibody Targeting the Interaction of PvDBP with Its Receptor DARC**

(A) Mice were infected with 0.87 million *P. vivax* sporozoites. Immunomodulation was performed as described in Figure 1A. On day 8, mice were randomized into two groups. Four mice were intraperitoneally injected with 100 mg/kg anti-PvDBP. Four mice served as controls, of which two were injected with 100 mg/kg anti-*P. yoelii* CSP and two mice were injected with 200  $\mu$ L PBS. Enriched reticulocytes were injected intravenously on days 9 and 10 post infection.

(B) Thin blood smears were performed 5 h after the second reticulocyte injection (d10pi) and 24 h after the second reticulocyte injection (d11pi). Infected red blood cells were enumerated in 50 fields. The control mice showed a mean of 67.5 parasites on day 10pi, whereas no parasites were seen in the group of mice passively transferred with anti-PvDBP. On day 11pi, one parasite was seen in one of the mice treated with anti-PvDBP, whereas the other three mice of this group remained blood smear negative. Each dot represents one mouse. Mean is shown. Statistics: unpaired t test; \*\*\* $p = 0.0001$ ; \*\* $p = 0.0037$ .

(C) IFAs were performed on thin blood smears from day 10pi, staining for human CD235a. Thousand cells were counted per slide, and the percentage of human red blood cells was calculated. There was no significant difference between the groups. Shown is mean with SD.

See also Figure S2.

liver stage development with the transition of exo-erythrocytic merozoites to blood stage infection. These features cannot currently be modeled *in vitro*. The unique advantage of this model over the existing *ex vivo* invasion assay (Russell et al., 2011) is that it provides the exclusive opportunity to test viability and infectivity of exo-erythrocytic merozoites and interventions that block the first stage of red blood cell infection by the parasite. The reproducibility of the described protocol for five different field isolates is especially remarkable and highlights the utility of this model.

To date, the only *in vivo* model system for *P. vivax* blood stages has been the non-human primate (NHP) model. *Aotus* or *Saimiri* species are susceptible to infection with NHP-adapted strains of *P. vivax* (Joyner et al., 2015). Although these models can produce informative data, there are difficulties that arise with their use. First, research using NHPs is limited owing to ethical concerns. The advancement of alternative model systems should greatly reduce the need to use NHPs for research purposes. Second, NHPs are not susceptible to infection with *P. vivax* field isolates. The parasite strains used for NHP studies had to be adapted in order to allow replication. It is unknown to what extent the biological features of these adapted strains are equivalent to *P. vivax* field isolates. For example, recent *de novo* assembly of a *P. vivax* field isolate genome identified large genomic regions including predicted protein-coding genes implicated to play a role in RBC invasion that were absent in the Sall adapted reference strain, which has been passaged extensively in NHPs (Hester et al., 2013).

Throughout our experiments, three different sources of blood were used, namely, cord blood, peripheral blood from healthy donors, and blood from patients with hemochromatosis. Although in our experiments reticulocytes from all three sources were invaded by merozoites with comparable efficiency, there are differences that need to be considered when deciding which blood source to use. Cord blood typically has higher reticulocyte counts but is expensive, and the volumes obtained are generally low. Furthermore, earlier reports suggested that *Plasmodium* parasites do not develop normally in red blood cells containing fetal hemoglobin (Wilson et al., 1977). These data have been challenged by more recent study results that show that *P. falciparum* and *P. vivax* parasites invade cord blood-derived RBCs as well as RBCs from peripheral blood (Archer et al., 2019; Roobsoong et al., 2015). Concordantly, the invasion capacity of the parasites in our model was not reduced in reticulocytes originating from cord blood. Conversely, obtaining access to large volumes of peripheral blood from healthy donors is facile, but reticulocyte counts are typically low. Therefore, we used blood from hemochromatosis patients. These patients undergo frequent phlebotomy as a treatment for iron overload disease and therefore have increased reticulocyte counts. Blood volumes of about 500 mL are drawn, making this an ideal source for large volumes of reticulocyte-rich blood.

Stage transition is a powerful feature of a model to test *P. vivax* erythrocytic vaccine candidates. In order to prevent disease and transmission, an erythrocytic stage vaccine ideally would not only prevent continuous blood stage infection but should effectively prevent the onset of asexual blood stage infection by blocking the first generation of merozoites that egress from the liver. Stage transition cannot robustly be modeled *in vitro* and is therefore a unique advantage of the described model over current *ex vivo* models. To this end, we used the FRGN KO huHep/huRetic model to test a monoclonal antibody against the interaction of the leading blood stage vaccine candidate PvDBP with its receptor DARC. We show that this antibody potently blocks the first wave of reticulocyte invasion by exo-erythrocytic merozoites, which proves the system highly suitable to test blood stage interventions. Although the *ex vivo* invasion assay described by Russell et al. (2011) provides the opportunity to test invasion inhibitory potential of antibodies, it has clearly been demonstrated that *in vitro* inhibitory activity of antibodies does not necessarily correlate with inhibitory activity seen *in vivo* (Kisalu et al., 2018; Sack et al., 2017). Therefore, the *in vivo* model described here is an important advance over the available *ex vivo* invasion assay.

Natural and experimental infections of humans have shown that *P. vivax* gametocytes are detectable as early as 3 days post onset of blood stage parasitemia. These observations have led to the hypothesis that a subset of *P. vivax* liver stage schizonts are pre-programmed to become gametocytes and therefore sexual stages already emerge with the first round of parasites egressing from the liver, allowing transmission before the onset of clinical symptoms (Bousema and Drakeley, 2011). Furthermore, gene expression data combined with mathematical modeling suggest that *P. vivax* transmission to mosquitoes is possible at the very first blood stage cycle and can therefore only be prevented if the first erythrocytic infection step is blocked (Adapa et al., 2019). Here, we provide the first direct *in vivo* evidence that a subset of exo-erythrocytic schizonts express the sexual stage marker Pvs16, but not the mature gametocyte marker Pvs230, and therefore exo-erythrocytic merozoites might be preprogrammed to become gametocytes in the first cycle of blood stage infection. This is in accordance with recent *in vitro* data in which infection of primary human hepatocytes with *P. vivax* sporozoites revealed Pvs16-expression on liver stage schizonts 8 days post infection (Roth et al., 2018). Importantly, the onset of blood stage parasitemia in the FRGN KO huHep/huRetic model further allowed us to follow the expression of gametocyte markers in erythrocytic stages. We detected Pvs16-expression on a subset of erythrocytic stage parasites as early as  $\leq 2$  days post onset of blood stage infection, suggesting that sexual stages can emerge within the first intra-erythrocytic replication cycle. Pvs16 is expressed early in gametocytogenesis and in line with the detection of Pvs16-expressing parasites  $\leq 2$  days post onset of blood stage infection, we observed gametocytes by Giemsa stain 1 day later, starting 3 days post onset of blood stage infection. Blocking liver to blood transition of *P. vivax* as demonstrated herein might thus offer the additional benefit of preventing parasite transmission. Clearly, these findings are of epidemiological importance and provide an intriguing example of the broad applicability of the FRGN KO huHep/huRetic model to answer highly translational as well as basic biological questions.

Future studies will be aimed at utilizing the *P. vivax* humanized mouse model to test not only erythrocytic but also pre-erythrocytic stage intervention strategies. The FRGN KO huHep/huRetic model will allow assessment of passive immunization against pre-erythrocytic stages by determining parasite liver burden, but importantly, it will also allow measurement of the onset of blood stage patency and the delay or absence thereof as an additional, highly sensitive readout for the efficacy of a pre-erythrocytic intervention.

It is questionable whether a single-stage subunit vaccine alone will be able to completely prevent infection, and thus, combination multi-stage vaccine approaches have to be considered (Tham et al., 2017). Since the FRGN KO huHep/huRetic model combines the natural route of infection, liver stage development and transition to parasite blood stages, it will provide the unique opportunity to test combination pre-erythrocytic stage and blood stage vaccine approaches, for which to date there is no available assay system.

In summary, we have developed a novel humanized mouse system that will serve as a valuable preclinical model to test interventions against *P. vivax* and will contribute to the accelerated discovery and development of novel vaccine and drug candidates.

### Limitations of the Study

The liver-chimeric mouse model described here is a highly specialized mouse model that requires careful handling owing to its immunocompromised nature. The additional depletion of mouse macrophages and mouse neutrophils with Clodronate liposomes and Cyclophosphamide makes the mice increasingly susceptible to bacterial infections, if not handled with required care.

Any work utilizing *P. vivax* sporozoites is challenging owing to the requirement of patient blood to infect mosquitoes in order to obtain these stages. This requires great logistical effort by laboratories in endemic countries. This, together with the complex nature of the mouse model used, requires careful assessment of the minimal group size necessary to achieve statistical significance.

The described model is a powerful tool for the transition of *P. vivax* liver stage to blood stage infection and testing of interventions against the first generation of merozoites egressing from the liver *in vivo*. Further refinement of the model will potentially allow continuous maintenance of asexual blood stage infection as well as parasite transmission to mosquitoes.

### Resource Availability

#### Lead Contact

Further information and requests for resources and reagents should be directed to and will be fulfilled by the Lead Contact, Stefan Kappe ([stefan.kappe@seattlechildrens.org](mailto:stefan.kappe@seattlechildrens.org)).

#### Materials Availability

The study did not generate new unique reagents.

#### Data and Code Availability

Any data generated in this study is included in the published article.

## METHODS

All methods can be found in the accompanying [Transparent Methods supplemental file](#).

## SUPPLEMENTAL INFORMATION

Supplemental Information can be found online at <https://doi.org/10.1016/j.isci.2020.101381>.

## ACKNOWLEDGMENTS

We thank the insectary team at Mahidol University for the supply of *P. vivax* infected mosquitoes and Yecuris Corp. for providing FRGN KO huHep mice. We thank Bloodworks Northwest and all donors for providing cord blood and blood units from patients with hemochromatosis. We also thank John Adams for the MSP1 antibody and Tomoko Ishino for Pvs16 and Pvs230 polyclonal serum. We thank Dr. Ashley Vaughan for critical reading of the manuscript and helpful discussions.

This work was funded by the German Research Foundation (fellowship SCHA2047/1-1 to CS) as well as the U.S. Department of Defense (award #W81XWH-17-1-0482 to SAM) and in part by the UK Medical Research Council (MRC) Confidence in Concept (MC\_PC\_16056) to M.B. T.A.R. held a Wellcome Trust Research Training Fellowship (108734/Z/15/Z), and S.J.D. is a Jenner Investigator and a Wellcome Trust Senior Fellow (106917/Z/15/Z).

## AUTHOR CONTRIBUTIONS

C.S. planned, performed, and analyzed experiments and wrote the manuscript; W.R. and N.K. performed experiments and analyzed data; M.B., T.A.R., and S.J.D. generated and provided the anti-DBP antibody biologic; D.N.S., O.T., and N.D. provided the anti-PyCSP control antibody and performed and analyzed ELISAs to determine serum antibody concentrations; C.P. and S.C.M. performed qRT-PCR analysis; D.G., L.M.R., and S.Y.K. performed laboratory work; W.R., N.K., and J.S. provided *P. vivax*-infected mosquitos; E.L.F., S.A.M., J.S., and S.H.I.K. supervised the work, analyzed data, and contributed to discussions; S.H.I.K. edited the manuscript; the final manuscript was edited and approved by all authors.

## DECLARATION OF INTERESTS

The authors declare no competing interests.

Received: February 6, 2020

Revised: April 2, 2020

Accepted: July 15, 2020

Published: August 21, 2020

## REFERENCES

- Adams, J.H., and Mueller, I. (2017). The biology of *Plasmodium vivax*. *Cold Spring Harb Perspect. Med.* 7, a025585.
- Adapa, S.R., Taylor, R.A., Wang, C., Thomson-Luque, R., Johnson, L.R., and Jiang, R.H.Y. (2019). *Plasmodium vivax* readiness to transmit: implication for malaria eradication. *BMC Syst. Biol.* 13, 5.
- Aikawa, M., Miller, L.H., and Rabbege, J. (1975). Caveola-vesicle complexes in the plasmalemma of erythrocytes infected by *Plasmodium vivax* and *P. cynomolgi*. Unique structures related to Schuffner's dots. *Am. J. Pathol.* 79, 285–300.
- Archer, N.M., Petersen, N., and Duraisingh, M.T. (2019). Fetal hemoglobin does not inhibit *Plasmodium falciparum* growth. *Blood Adv.* 3, 2149–2152.
- Armistead, J.S., and Adams, J.H. (2018). Advancing research models and technologies to overcome biological barriers to *Plasmodium vivax* control. *Trends Parasitol.* 34, 114–126.
- Azuma, H., Paulk, N., Ranade, A., Dorrell, C., Al-Dhalimy, M., Ellis, E., Strom, S., Kay, M.A., Finegold, M., and Grompe, M. (2007). Robust expansion of human hepatocytes in Fah<sup>-/-</sup>/Rag2<sup>-/-</sup>/Il2rg<sup>-/-</sup> mice. *Nat. Biotechnol.* 25, 903–910.
- Bass, C.C., and Johns, F.M. (1912). The cultivation of malarial plasmodia (*Plasmodium vivax* and *Plasmodium falciparum*) in vitro. *J. Exp. Med.* 16, 567–579.
- Bermudez, M., Moreno-Perez, D.A., Arevalo-Pinzon, G., Curtidor, H., and Patarroyo, M.A. (2018). *Plasmodium vivax* in vitro continuous culture: the spoke in the wheel. *Malar. J.* 17, 301.
- Bousema, T., and Drakeley, C. (2011). Epidemiology and infectivity of *Plasmodium falciparum* and *Plasmodium vivax* gametocytes in relation to malaria control and elimination. *Clin. Microbiol. Rev.* 24, 377–410.
- Cowell, A.N., and Winzeler, E.A. (2019). Advances in omics-based methods to identify novel targets for malaria and other parasitic protozoan infections. *Genome Med.* 11, 63.
- de Cassan, S.C., Shakri, A.R., Llewellyn, D., Elias, S.C., Cho, J.S., Goodman, A.L., Jin, J., Douglas, A.D., Suwanarusk, R., Nosten, F.H., et al. (2015). Preclinical assessment of viral vectored and protein vaccines targeting the duffy-binding protein region II of *Plasmodium vivax*. *Front. Immunol.* 6, 348.
- Foquet, L., Schafer, C., Minkah, N.K., Alanine, D.G.W., Flannery, E.L., Steel, R.W.J., Sack, B.K., Camargo, N., Fishbaugher, M., Betz, W., et al. (2018). *Plasmodium falciparum* liver stage infection and transition to stable blood stage infection in liver-humanized and blood-humanized FRGN KO mice enables testing of blood stage inhibitory antibodies (Reticulocyte-Binding protein homolog 5) in vivo. *Front. Immunol.* 9, 524.
- Gething, P.W., Van Boeckel, T.P., Smith, D.L., Guerra, C.A., Patil, A.P., Snow, R.W., and Hay, S.I. (2011). Modelling the global constraints of temperature on transmission of *Plasmodium falciparum* and *P. vivax*. *Parasit. Vectors* 4, 92.
- Goswami, D., Minkah, N.K., and Kappe, S.H.I. (2019). Designer parasites: genetically engineered *Plasmodium* as vaccines to prevent malaria infection. *J. Immunol.* 202, 20–28.
- Grimberg, B.T., Udamsangpetch, R., Xainli, J., McHenry, A., Panichakul, T., Sattabongkot, J., Cui, L., Bockarie, M., Chitnis, C., Adams, J., et al. (2007). *Plasmodium vivax* invasion of human erythrocytes inhibited by antibodies directed against the Duffy binding protein. *PLoS Med.* 4, e337.
- Gruszczyk, J., Kanjee, U., Chan, L.J., Menant, S., Malleret, B., Lim, N.T.Y., Schmidt, C.Q., Mok, Y.F., Lin, K.M., Pearson, R.D., et al. (2018). Transferrin receptor 1 is a reticulocyte-specific receptor for *Plasmodium vivax*. *Science* 359, 48–55.
- He, W.Q., Shakri, A.R., Bhardwaj, R., Franca, C.T., Stanicic, D.I., Healer, J., Kiniboro, B., Robinson, L.J., Guillotte-Blisnick, M., Huon, C., et al. (2019). Antibody responses to *Plasmodium vivax* Duffy binding and Erythrocyte binding proteins predict risk of infection and are associated with protection from clinical Malaria. *PLoS Negl. Trop. Dis.* 13, e0006987.
- Hester, J., Chan, E.R., Menard, D., Mercereau-Pujalon, O., Barnwell, J., Zimmerman, P.A., and Serre, D. (2013). De novo assembly of a field isolate genome reveals novel *Plasmodium vivax* erythrocyte invasion genes. *PLoS Negl. Trop. Dis.* 7, e2569.
- Joyner, C., Barnwell, J.W., and Galinski, M.R. (2015). No more monkeying around: primate malaria model systems are key to understanding *Plasmodium vivax* liver-stage biology, hypnozoites, and relapses. *Front. Microbiol.* 6, 145.
- King, C.L., Michon, P., Shakri, A.R., Marcotty, A., Stanicic, D., Zimmerman, P.A., Cole-Tobian, J.L., Mueller, I., and Chitnis, C.E. (2008). Naturally acquired Duffy-binding protein-specific binding inhibitory antibodies confer protection from blood-stage *Plasmodium vivax* infection. *Proc. Natl. Acad. Sci. U S A* 105, 8363–8368.
- Kisalu, N.K., Idris, A.H., Weidle, C., Flores-Garcia, Y., Flynn, B.J., Sack, B.K., Murphy, S., Schon, A., Freire, E., Francica, J.R., et al. (2018). A human monoclonal antibody prevents malaria infection by targeting a new site of vulnerability on the parasite. *Nat. Med.* 24, 408–416.
- Kwong, L.S., Brown, M.H., Barclay, A.N., and Hatherley, D. (2014). Signal-regulatory protein alpha from the NOD mouse binds human CD47 with an exceptionally high affinity—implications for engraftment of human cells. *Immunology* 143, 61–67.
- Liehl, P., Meireles, P., Albuquerque, I.S., Pinkevych, M., Baptista, F., Mota, M.M., Davenport, M.P., and Prudencio, M. (2015). Innate immunity induced by *Plasmodium* liver infection inhibits malaria reinfections. *Infect. Immun.* 83, 1172–1180.
- Malleret, B., Li, A., Zhang, R., Tan, K.S., Suwanarusk, R., Claser, C., Cho, J.S., Koh, E.G., Chu, C.S., Pukrittayakamee, S., et al. (2015). *Plasmodium vivax*: restricted tropism and rapid

remodeling of CD71-positive reticulocytes. *Blood* 125, 1314–1324.

Mikolajczak, S.A., Vaughan, A.M., Kangwanrangsang, N., Roobsoong, W., Fishbaugher, M., Yimamnuaychok, N., Rezakhani, N., Lakshmanan, V., Singh, N., Kaushansky, A., et al. (2015). *Plasmodium vivax* liver stage development and hypnozoite persistence in human liver-chimeric mice. *Cell Host Microbe* 17, 526–535.

Miller, J.L., Sack, B.K., Baldwin, M., Vaughan, A.M., and Kappe, S.H.I. (2014). Interferon-mediated innate immune responses against malaria parasite liver stages. *Cell Rep.* 7, 436–447.

Mogire, R.M., Akala, H.M., Macharia, R.W., Juma, D.W., Cheruiyot, A.C., Andagalu, B., Brown, M.L., El-Shemy, H.A., and Nyanjom, S.G. (2017). Target-similarity search using *Plasmodium falciparum* proteome identifies approved drugs with anti-malarial activity and their possible targets. *PLoS One* 12, e0186364.

Moreno, A., Caro-Aguilar, I., Yazdani, S.S., Shakri, A.R., Lapp, S., Strobert, E., McClure, H., Chitnis, C.E., and Galinski, M.R. (2008). Preclinical assessment of the receptor-binding domain of *Plasmodium vivax* Duffy-binding protein as a vaccine candidate in rhesus macaques. *Vaccine* 26, 4338–4344.

Ney, P.A. (2011). Normal and disordered reticulocyte maturation. *Curr. Opin. Hematol.* 18, 152–157.

Noulin, F., Borlon, C., Van Den Abbeele, J., D'Alessandro, U., and Erhart, A. (2013). 1912–2012: a century of research on *Plasmodium vivax* in vitro culture. *Trends Parasitol.* 29, 286–294.

Payne, R.O., Silk, S.E., Elias, S.C., Milne, K.H., Rawlinson, T.A., Llewellyn, D., Shakri, A.R., Jin, J., Labbe, G.M., Edwards, N.J., et al. (2017). Human vaccination against *Plasmodium vivax* Duffy-

binding protein induces strain-transcending antibodies. *JCI Insight* 2, e93683.

Rawlinson, T.A., Barber, N.M., Mohring, F., Cho, J.S., Kosaisavee, V., Gerard, S.F., Alanine, D.G.W., Labbe, G.M., Elias, S.C., Silk, S.E., et al. (2019). Structural basis for inhibition of *Plasmodium vivax* invasion by a broadly neutralizing vaccine-induced human antibody. *Nat. Microbiol.* 4, 1497–1507.

Roobsoong, W., Tharinjaroen, C.S., Rachaphaew, N., Chobson, P., Schofield, L., Cui, L., Adams, J.H., and Sattabongkot, J. (2015). Improvement of culture conditions for long-term in vitro culture of *Plasmodium vivax*. *Malar. J.* 14, 297.

Roth, A., Maher, S.P., Conway, A.J., Ubalee, R., Chaumeau, V., Andolina, C., Kaba, S.A., Vantaux, A., Bakowski, M.A., Thomson-Luque, R., et al. (2018). A comprehensive model for assessment of liver stage therapies targeting *Plasmodium vivax* and *Plasmodium falciparum*. *Nat. Commun.* 9, 1837.

Russell, B., Suwanarusk, R., Borlon, C., Costa, F.T., Chu, C.S., Rijken, M.J., Sriprawatt, K., Warter, L., Koh, E.G., Malleret, B., et al. (2011). A reliable ex vivo invasion assay of human reticulocytes by *Plasmodium vivax*. *Blood* 118, e74–e81.

Sack, B.K., Mikolajczak, S.A., Fishbaugher, M., Vaughan, A.M., Flannery, E.L., Nguyen, T., Betz, W., Jane Navarro, M., Foquet, L., Steel, R.W.J., et al. (2017). Humoral protection against mosquito bite-transmitted *Plasmodium falciparum* infection in humanized mice. *NPJ Vaccin.* 2, 27.

Shretta, R., Liu, J., Cotter, C., Cohen, J., Dolenz, C., Makomva, K., Newby, G., Menard, D., Phillips, A., Tatarsky, A., et al. (2017). Malaria elimination and eradication; Chapter 12. In *Major Infectious Diseases*, 3rd ed. K.K. Holmes, S. Bertozzi, B.R. Bloom, and P. Jha, eds. (The International Bank

for Reconstruction and Development / The World Bank).

Singh, K., Mukherjee, P., Shakri, A.R., Singh, A., Pandey, G., Bakshi, M., Uppal, G., Jena, R., Rawat, A., Kumar, P., et al. (2018). Malaria vaccine candidate based on Duffy-binding protein elicits strain transcending functional antibodies in a Phase I trial. *NPJ Vaccin.* 3, 48.

Suwanarusk, R., Cooke, B.M., Dondorp, A.M., Silamut, K., Sattabongkot, J., White, N.J., and Udomsangpetch, R. (2004). The deformability of red blood cells parasitized by *Plasmodium falciparum* and *P. vivax*. *J. Infect. Dis.* 189, 190–194.

Tham, W.H., Beeson, J.G., and Rayner, J.C. (2017). *Plasmodium vivax* vaccine research - we've only just begun. *Int. J. Parasitol.* 47, 111–118.

Trager, W. (1977). Cultivation of *Plasmodium falciparum*. *Arch. Pathol. Lab. Med.* 101, 277–278.

White, M.T., Karl, S., Battle, K.E., Hay, S.I., Mueller, I., and Ghani, A.C. (2014). Modelling the contribution of the hypnozoite reservoir to *Plasmodium vivax* transmission. *Elife* 3, e04692.

White, N.J. (2011). Determinants of relapse periodicity in *Plasmodium vivax* malaria. *Malar. J.* 10, 297.

Wilson, R.J., Pasvol, G., and Weatherall, D.J. (1977). Invasion and growth of *Plasmodium falciparum* in different types of human erythrocyte. *Bull. World Health Organ.* 55, 179–186.

Yamauchi, T., Takenaka, K., Urata, S., Shima, T., Kikushige, Y., Tokuyama, T., Iwamoto, C., Nishihara, M., Iwasaki, H., Miyamoto, T., et al. (2013). Polymorphic Sirpa is the genetic determinant for NOD-based mouse lines to achieve efficient human cell engraftment. *Blood* 121, 1316–1325.

## **Supplemental Information**

### **A Humanized Mouse Model for *Plasmodium vivax* to Test Interventions that Block Liver Stage to Blood Stage Transition and Blood Stage Infection**

**Carola Schäfer, Wanlapa Roobsoong, Niwat Kangwanransan, Martino Bardelli, Thomas A. Rawlinson, Nicholas Dambrauskas, Olesya Trakhimets, Chaitra Parthiban, Debashree Goswami, Laura M. Reynolds, Spencer Y. Kennedy, Erika L. Flannery, Sean C. Murphy, D. Noah Sather, Simon J. Draper, Jetsumon Sattabongkot, Sebastian A. Mikolajczak, and Stefan H.I. Kappe**

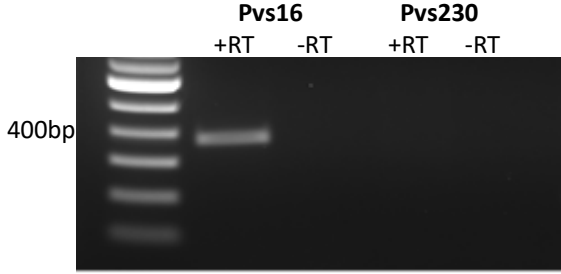


**Figure S1. Detection of Pvs16 expression by RT-PCR, Related to Figure 3**

RNA was isolated from *P. vivax* infected FRG KO huHep livers eight days post sporozoite infection. Following reverse transcription, Pvs16 transcript was successfully detected by PCR, confirming the expression of Pvs16 by *P. vivax* liver stages, whereas we were not able to detect expression of the mature gametocyte marker Pvs230. +RT=with reverse transcriptase;

-RT=without reverse transcriptase.

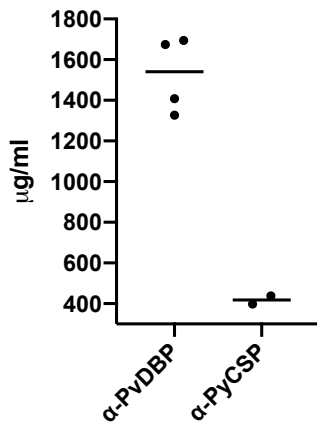


**Figure S2. High serum antibody levels were detected before reticulocyte injection, Related to Figure 4**

Serum antibody levels were measured by ELISA on day 9 post infection, directly before the first reticulocyte injection and revealed high antibody concentrations. Each dot represents one mouse and median is shown.

## **Transparent Methods**

### **Ethics statement**

The Human Subjects Protocol for this study was approved by the Ethical Review Committee of the Faculty of Tropical Medicine, Mahidol University.

All animal experiments were carried out in accordance with the recommendations of the NIH Office of Laboratory Animal Welfare standards. Mice were maintained under specific pathogen-free conditions at the Center for Global Infectious Disease Research, Seattle Children's Research Institute. The protocol was approved by the Center for Infectious Disease Research Institutional Animal Care and Use Committee (IACUC) under protocol 00480.

### **Mice**

Female FRGN KO huHep mice were purchased from Yecuris Inc. Serum albumin levels of all mice used exceeded 4mg/ml, corresponding to >70% human hepatocyte repopulation. Mice were maintained on drinking water containing 3% Dextrose and were cycled on 8 mg/L NTBC once a month for 4 days to maintain hepatocyte chimerism.

### **Infection of FRGN KO huHep mice with *P. vivax* sporozoites and mAb passive transfer**

All sporozoites were obtained by microdissection of salivary glands from mosquitoes that had been fed on *P. vivax* infected blood obtained from patients seeking treatment for *P. vivax* malaria at malaria clinics along the Thai–Myanmar border. 14–16 days after the blood meal, mosquito salivary glands were dissected and sporozoites were collected into cold Schneider's insect media (Sigma Aldrich). Salivary glands were crushed and sporozoites were enumerated using a hemocytometer. 0.6 – 0.9 million sporozoites were injected intravenously into FRGN KO huHep mice. To prevent bacterial coinfections, mice were injected intraperitoneally with 1000 Units Penicillin and 1mg Streptomycin (Sigma Aldrich) every other day after the infection.

We tested a modified version of the reported human DB9 monoclonal antibody, targeting the essential PvDBP-DARC interaction (Rawlinson et al., 2019), which is referred to in the text as “anti-PvDBP”. 100 mg/kg of this antibody, an antibody against PyCSP as off-target control or 100ul PBS were injected intraperitoneally 24 hours prior to the first reticulocyte injection.

### **Enrichment of reticulocytes from whole blood and reticulocyte repopulation of FRGN KO huHep mice**

Blood was collected either from the umbilical cord directly after delivery of a child, or by phlebotomy of healthy donors or patients with hemochromatosis. All blood collections were performed at Bloodworks NW. CPDA was used as anticoagulant. The blood was leuko-reduced using a Leukocyte reduction filter (Haemonetics Corp. MA, USA) and subsequently washed three times in RPMI 1640 (25 mM HEPES, 2 mM L-glutamine; Sigma Aldrich) to deplete any remaining white blood cells. Packed RBCs were resuspended in RPMI1640 to 20% hematocrit. 4ml of this RBC preparation was layered on top of 4ml 25% OptiPrep™ in PBS (Stemcell Technologies Inc., USA) and centrifuged at 3000xg for 30 mins without brake. The resulting layer of enriched reticulocytes was washed three times in RPMI1640 and stored in McCoy's 5A media (Thermo Fisher Scientific, USA) at 4°C for a maximum of 5 days. Reticulocyte content was determined by New Methylene Blue staining and reticulocyte preparations contained 30 - 60% reticulocytes. On days 3, 7 and 10 post infection, mice received 150ul or 100ul respectively of Clodronate liposomes (Chlophosome®-A; FormuMax) and 150mg/kg Cyclophosphamide (Sigma Aldrich) intraperitoneally. After two reticulocyte injections on days 9 and 10 post infection, mice reached about 30% red blood cell chimerism. Assuming that 30 - 60% of the human cells injected are reticulocytes, mice had between 9 and 18% human reticulocytes of the total red blood cells available for invasion by the parasite. The number of invaded cells is shown as % parasitemia.

Notably, this parasitemia is measured as a percentage of total red blood cells, including mouse cells.

### **18S rRNA qRT-PCR quantification of parasite load**

On day 10 post infection, 5 hours after the second reticulocyte injection, 50ul blood was drawn, immediately added to 1ml NucliSENS Lysis buffer (bioMérieux, Marcy-l'Étoile, France) and frozen at -80°C. The samples were processed and analyzed for presence of *Plasmodium* 18S rRNA using a pan-*Plasmodium* probe as previously described (Seilie et al., 2019).

### **Immunofluorescence assays of liver sections**

After harvest, liver samples were fixed in 4% Paraformaldehyde over night at room temperature. After two washes in 1xTBS they were sliced to 50µm sections using a vibratome. Subsequent incubations were performed on a shaker set to 80rpm. Liver sections were permeabilized in 10% H<sub>2</sub>O<sub>2</sub> and 0.25% Triton X-100 in 1xTBS for 30 minutes at room temperature. After one wash in 1xTBS sections were blocked in 5% skim milk in 1xTBS for one hour at room temperature before incubating overnight at 4°C with anti-Pvs16 or anti-Pvs230 (rabbit polyclonal serum, kindly provided by Tomoko Ishino, Ehime University, Japan) diluted 1:200 in 5% skim milk and anti-UIS4 mouse monoclonal (Schafer et al., 2018) diluted 1:500 in 5% skim milk. Liver sections were subjected to three five-minute washes before addition of 2µg/ml Alexa Fluor-488 labeled goat anti-mouse IgG and 2µg/ml Alexa Fluor-594 labeled goat anti-rabbit IgG (Thermo Fisher) and incubation for two hours at room temperature. After one five-minute wash in 1xTBS, sections were transferred to 1xTBS containing 2µg/ml DAPI and incubated for 10 minutes at room temperature, before washing again in 1xTBS. To reduce background fluorescence, sections were incubated for ~20 seconds in 0.06% KMnO<sub>4</sub> in 1xTBS before washing one more time in 1xTBS and mounting on a poly-Lysine coated slide using ProLong™ Gold Antifade mounting solution (ThermoFisher)

to preserve fluorescence before analysis and image acquisition using Olympus 1x70 DeltaVision deconvolution microscopy.

### **RT-PCR to detect Pvs16 and Pvs230 transcript in mouse liver samples**

FRG KO huHep mice were infected with one million *P. vivax* sporozoites. On day 8 post infection, livers were harvested, each liver lobe was cut in half and all lobes from each mouse were pooled together in TRIzol reagent (Invitrogen). Livers were homogenized and RNA was extracted using the RNeasy purification kit (Qiagen). RNA was reverse transcribed to cDNA using the Primescript RT reagent kit (Takara) prior to PCR using BioMix (Bioline) and primers specific to Pvs16 (primer sequences: fwd: TCCTCTTGTGTGTCCTGCTAA rev: CCCCTTTTGGGCTTCTGGA Product size: 374 bp ) or Pvs230 (Primer sequences: fwd: 5'- CGCCAAGCAGACGGATGATA -3'; rev: 5'- GTCCTCCGTGGATTGCTCATC -3'; Product size: 526 bp).

### **Immunofluorescence assays of thin blood smears**

Thin blood smears were obtained from infected mice and fixed in pre-chilled Methanol for four minutes. Slides were washed once in PBS before blocking with 4% BSA in PBS for one hour at room temperature. Incubation with primary antibodies was performed in 1% BSA in PBS at 4°C overnight after which slides were washed three times in PBS. Anti-mouse or anti-rabbit secondary antibodies conjugated to Alexa Fluor 488 or 594 were applied at 1:500 dilution in 1% BSA in PBS together with DAPI (1:1000) to visualize DNA. Slides were incubated for 1 hour at RT after which they were washed three times in 1xPBS. One drop of ProLong™ Gold Antifade mounting solution (ThermoFisher) was added to preserve fluorescence before applying the cover slip.

Primary antibodies used are: rabbit polyclonals against Pvs16 at 1:200 dilution (kindly provided by Tomoko Ishino, Ehime University, Japan); mouse monoclonal against MSP1 at 1:100 dilution

(kindly provided by John Adams, University of South Florida, USA); mouse anti-CD235a at 1:100 dilution (Biorbyt, USA); rabbit anti-*Plasmodium* BiP at 1:200 dilution.

All images were acquired using Olympus 1x70 DeltaVision deconvolution microscopy.

### **Quantification of serum antibody levels by ELISA**

All serum samples were heat-inactivated for 30 minutes at 56 °C prior to any assays, run with duplicate wells and confirmed in duplicate assays. To determine serum anti-PvDBP antibody concentrations, Immulon 2HB 96-well plates (Thermo Scientific, 3455) were coated with 200 ng per well of rabbit anti-human IgG antibody (Invitrogen, SA510223) overnight in 0.1M NaHCO<sub>3</sub>, pH 9.5. In all assays, plates were washed between each ELISA step with PBS, 0.2% Tween-20 and incubations were 1 hour at 37°C. Coated plates were blocked with PBS, 10% non-fat milk, and 0.3% Tween-20. Following blocking, serum was serially diluted over a range of 1:200 to 1:11,809,800 and purified recombinant anti-PvDBP over a range of 1 to 0.000017 µg/ml in PBS, 10% non-fat milk, and 0.03% Tween-20. Bound antibodies were detected using goat anti-human IgG (H+L)-HRP (Invitrogen, A18811) at 1:1000 dilution in PBS, 10% non-fat milk, and 0.03% Tween-20. To determine serum anti-PyCSP antibody concentrations, plates were coated with 50 ng per well of Streptavidin (New England Biolabs, N7021S) in 0.1M NaHCO<sub>3</sub>, pH 9.5. Coated plates were blocked with PBS, 3% BSA, then coated with 200 ng per well of biotinylated PyCSP in PBS, 0.2% BSA. Plates were then blocked with PBS, 10% non-fat milk, and 0.3% Tween-20. Following blocking, serum was serially diluted over a range of 1:200 to 1:11,809,800 and purified anti-PyCSP antibody over a range of 0.5 to 0.000008 µg/ml in PBS, 0.2% BSA. Bound antibodies were detected using goat anti-mouse IgG Fc-HRP (Southern Biotech, 1013-05) at 1:2000 dilution in PBS and 0.2% BSA. All plates were developed with 50 µl of TMB Peroxidase Substrate (SeraCare Life Sciences Inc, 5120-0083) equilibrated to room temperature and stopped after 3

minutes with 50  $\mu$ l of 1N H<sub>2</sub>SO<sub>4</sub>. Absorbance at 450 nm was detected on a BioTek ELx800 microplate reader. Standard curves for anti-PvDBP or anti-PyCSP controls were generated by nonlinear regression (log[agonist] vs response[three parameters]) in GraphPad Prism V8 (San Diego, CA). Serum antibody concentrations were quantified by interpolating the average values from three different dilutions along the corresponding standard curves and multiplying by the dilution factor to determine the final concentration.

### **Statistical analysis**

Statistical analysis was carried out using GraphPad Prism version 8.3.1. The specific statistical tests performed for each experiment are included in the corresponding figure legend.

### **Supplemental References**

Rawlinson, T.A., Barber, N.M., Mohring, F., Cho, J.S., Kosaisavee, V., Gerard, S.F., Alanine, D.G.W., Labbe, G.M., Elias, S.C., Silk, S.E., *et al.* (2019). Structural basis for inhibition of *Plasmodium vivax* invasion by a broadly neutralizing vaccine-induced human antibody. *Nat Microbiol* *4*, 1497-1507.

Schafer, C., Dambrauskas, N., Steel, R.W., Carbonetti, S., Chuenchob, V., Flannery, E.L., Vigdorovich, V., Oliver, B.G., Roobsoong, W., Maher, S.P., *et al.* (2018). A recombinant antibody against *Plasmodium vivax* UIS4 for distinguishing replicating from dormant liver stages. *Malar J* *17*, 370.

Seilie, A.M., Chang, M., Hanron, A.E., Billman, Z.P., Stone, B.C., Zhou, K., Olsen, T.M., Daza, G., Ortega, J., Cruz, K.R., *et al.* (2019). Beyond Blood Smears: Qualification of *Plasmodium* 18S rRNA as a Biomarker for Controlled Human Malaria Infections. *Am J Trop Med Hyg* *100*, 1466-1476.